

# Effect of tetrahedral shapes in heavy and superheavy nuclei

P. Jachimowicz

*Institute of Physics, University of Zielona Góra, Szafrana 4a, 65-516 Zielona Góra, Poland*

M. Kowal\* and J. Skalski

*National Centre for Nuclear Research, Hoża 69, 00-681 Warsaw, Poland*

(Dated: January 30, 2017)

We search for effects of tetrahedral deformation  $\beta_{32}$  over a range of  $\sim 3000$  heavy and superheavy nuclei,  $82 \leq Z \leq 126$ , using a microscopic-macroscopic model based on the deformed Woods-Saxon potential, well tested in the region. We look for the energy minima with a non-zero tetrahedral distortion, both absolute and conditional - with the quadrupole distortion constrained to zero. In order to assure reliability of our results we include 10 most important deformation parameters in the energy minimization. We could not find any cases of stable tetrahedral shapes. The only sizable - up to 0.7 MeV - lowering of the ground state occurs in superheavy nuclei  $Z \geq 120$  for  $N = 173-188$ , as a result of a *combined* action of two octupole deformations:  $\beta_{32}$  and  $\beta_{30}$ , in the ratio  $\beta_{32}/\beta_{30} \approx \sqrt{3/5}$ . The resulting shapes are moderately oblate, with the superimposed distortion  $\beta_{33}$  *with respect to the oblate axis*, which makes the equator of the oblate spheroid slightly triangular. Almost all found conditional minima are excited and not protected by any barrier; a handful of them are degenerate with the axial minima.

## I. INTRODUCTION

The idea of intrinsic shape of a nucleus turned out instrumental for understanding many features of the nuclear structure and spectroscopy. In particular, specific nuclear shapes were related to the prominent shell effects in both proton and neutron systems exhibited by the nuclear binding, and to the observed patterns of collective excitations. Besides the axial quadrupole distortion which is the nuclear deformation of primary importance, the secondary effects of hexadecapole [1, 2] and, in some regions, octupole [3–5] distortion are clearly recognized. Additionally, there are theoretical predictions of quadrupole triaxial equilibrium shapes in some nuclei, e.g. [6, 7], but rather limited experimental evidence for them, see e.g. [8, 9]. From the theoretical point of view even more exotic shapes are possible, characterized by a high rank symmetry group which would lead to an extra degeneracy of s.p. energy levels. One such possibility is the tetrahedral symmetry. It is well known that many quantum objects, like molecules, fullerenes and alkali metal clusters prefer such a shape in their ground state. Due to these facts a hypothesis of tetrahedral symmetry of an atomic nucleus was put forward as early as in the 1970s for  $^{16}\text{O}$  [10, 11] in relation to its expected four- $\alpha$  cluster structure. Since the 1990s, such concept has been extended also to the heavier systems, e.g. [12, 13] and then intensively studied, both within microscopic-macroscopic (MM) [14–17, 24] and selfconsistent models [14, 15, 18–23]. Generally, these studies are inconclusive since: a) the existence of global tetrahedral minima was rare and model-dependent b) contradictory results were obtained within the same models. Similar ambiguity occurs also in experiments which so far either did not give a clear evidence [25] or even gave a strong evidence against tetrahedral symmetry [26, 27]. For example, negative-parity bands in  $^{156}\text{Dy}$ , observed quite recently [28], are most likely related to the octupole excitations rather than the exotic tetrahedral symmetry.

Here we summarize the results of a search for tetrahedral minima in heavy and super-heavy nuclei obtained within the MM model based on the deformed Woods-Saxon potential with parameters used many times before, therefore well tested in this region. The present work is a much improved version of [24], extended to odd- $A$  and odd-odd nuclei, with an expanded space of deformations used for searching ground-state (absolute) tetrahedral minima.

---

\*Electronic address: [michal.kowal@ncbj.gov.pl](mailto:michal.kowal@ncbj.gov.pl)

## II. CALCULATIONS

The microscopic-macroscopic results were obtained with the deformed Woods-Saxon potential. The nuclear deformation enters via a definition of the nuclear surface [29]:

$$R(\theta, \varphi) = c(\{\beta\})R_0\left\{1 + \sum_{\lambda>1} \beta_{\lambda 0} Y_{\lambda 0}(\theta, \varphi) + \sum_{\lambda>1, \mu>0, \text{even}} \beta_{\lambda \mu} Y_{\lambda \mu}^c(\theta, \varphi)\right\}, \quad (1)$$

where  $c(\{\beta\})$  is the volume-fixing factor. The real-valued spherical harmonics  $Y_{\lambda \mu}^c$ , with even  $\mu > 0$ , are defined in terms of the usual ones as:  $Y_{\lambda \mu}^c = (Y_{\lambda \mu} + Y_{\lambda -\mu})/\sqrt{2}$ . In other words, we consider shapes with two symmetry planes. Note, that traditional quadrupole deformations  $\beta$  and  $\gamma$  are related to  $\beta_{20}$  and  $\beta_{22}$  by:  $\beta_{20} = \beta \cos \gamma$  and  $\beta_{22} = \beta \sin \gamma$ .

The  $n_p = 450$  lowest proton levels and  $n_n = 550$  lowest neutron levels from the  $N_{max} = 19$  lowest shells of the deformed oscillator were taken into account in the diagonalization procedure. For the macroscopic part we used the Yukawa plus exponential model [30].

All parameters used in the present work, determining the s.p. potential, the pairing strength, and the macroscopic energy, are equal to those used previously in the calculations of masses [31] and fission barriers [32–34] in actinides and the heaviest nuclei. In particular, we took the "universal set" of potential parameters and the pairing strengths  $G_n = (17.67 - 13.11 \cdot I)/A$  for neutrons,  $G_p = (13.40 + 44.89 \cdot I)/A$  for protons ( $I = (N - Z)/A$ ). As always within this model,  $N$  neutron and  $Z$  proton s.p. levels have been included when solving BCS equations. For systems with odd proton or neutron (or both) we use blocking. We assume the g.s. configuration consisting of an odd particle occupying one of the levels close to the Fermi level and the rest of the particles forming a paired BCS state on the remaining levels. Any minimum, including the ground state, is found by minimizing over configurations, blocking particles on levels from the 10-th below to 10-th above the Fermi level.

We performed three types of calculations looking for both conditional and ground-state tetrahedral minima in nearly 3000 heavy and superheavy nuclei with  $Z \geq 82$ .

1) Conditional tetrahedral minima were found by fixing quadrupole deformations at zero:  $\beta_{20} = \beta_{22} = 0$ , and calculating total energy with the step 0.02 in  $\beta_{32}$  by minimization over the other seven deformation parameters:  $\beta_{30}, \beta_{40}, \beta_{42}, \beta_{50}, \beta_{60}, \beta_{70}, \beta_{80}$ . The occurrence of a minimum at  $\beta_{32} \neq 0$  in such an energy plot (after additional interpolation of the energy to the step 0.01 in  $\beta_{32}$ ) signals the conditional minimum, usually excited above the g.s. The rationale behind this procedure is that, as known from other studies, quadrupole deformation does not cooperate with the tetrahedral one [15, 16], and switching off the effects of the quadrupole might help to locate a prominent tetrahedral shell effect at sizable deformation  $\beta_{32}$ .

2) The ground states in all nuclei were found initially by the minimization over seven axial deformations  $\beta_{\lambda 0}$ ,  $\lambda = 2 - 8$ .

3) Finally, the ground states were found for the second time, by the minimization over ten deformations: the axial ones from 2) plus  $\beta_{22}, \beta_{32}$ , and  $\beta_{42}$ .

In additional calculations, for a restricted region of SH nuclei in which the minima found in 3) were  $\sim 0.5$  MeV deeper than those resulting from 2), we minimized energy with respect to nine deformations, excluding  $\beta_{32}$ . The aim was to see whether the effect is driven by  $\beta_{32}$ .

In all calculations we used one non-axial version of the WS code to eliminate possible numerical differences which could follow from the different imposed spatial symmetries. When looking for ground state minima, a minimization for each nucleus was repeated at least 30 times, with various starting points, in order to ensure that the proper ground state was found. As, especially for superheavy nuclei, the minimization can end behind the fission barrier, only minima within the the fission barrier were accepted.

## III. RESULTS AND DISCUSSION

### A. Tetrahedral minima

The map of tetrahedral deformations in the obtained conditional minima is shown in Fig. 1. We emphasize that in these minima the quadrupole deformation was forced to vanish in order to exhibit large tetrahedral shell effects. As may be seen, the largest  $\beta_{32}$  reach  $\sim 0.2$ . The conditional tetrahedral minima with sizable  $\beta_{32} > 0.1$  occur in three regions: a wide region around  $Z = 94$ ,  $N = 136$ , and two very exotic regions:  $Z \approx 98$ ,  $N \approx 192$ , and  $Z = 126$ ,  $N \approx 192$ . This, however, should be confronted with the excitation energies of the conditional minima above the axially

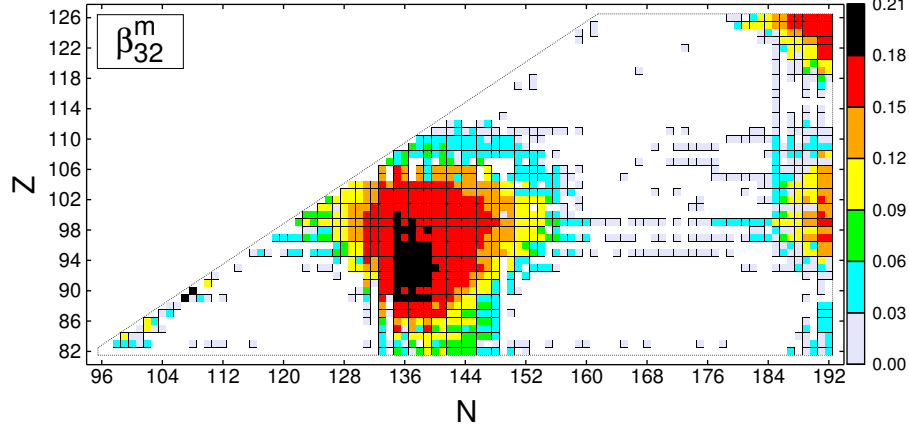


FIG. 1: (color online) Deformation  $\beta_{32}$  at the conditional minima obtained by setting  $\beta_{20} = \beta_{22} = 0$ ; the minimization performed over 7 other deformation parameters (see text).

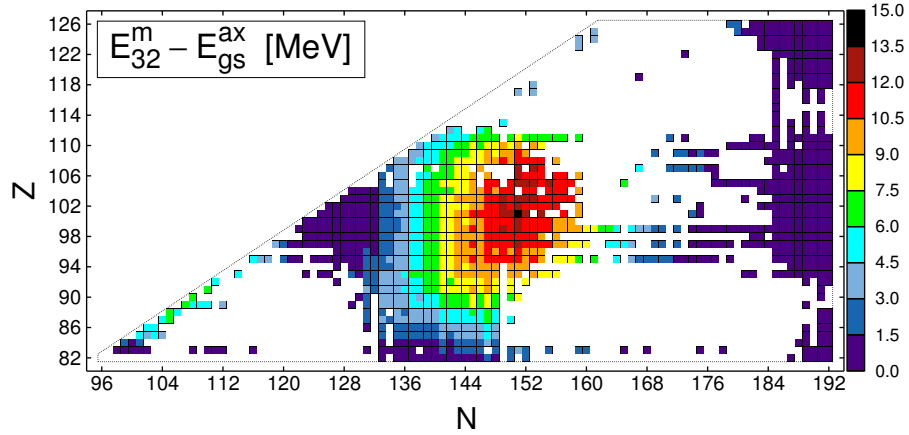


FIG. 2: (color online) Excitation energy of the conditional minima with  $\beta_{32} \neq 0$  above the axially symmetric g.s.

symmetric g.s. minima [found in calculations no. 2)], shown in Fig. 2. As may be seen there, the low excitation energies in the *a priori* interesting first region occur in neutron rich  $Z = 84 - 94$  nuclei and in the very neutron deficient  $Z = 92 - 106$  isotopes which probably cannot be reached in experiment. There are some very exotic nuclei in which the conditional tetrahedral minima lie lower than the axially symmetric ones, but the largest difference is only 0.25 MeV. The conclusion from this part of the study is that in the whole investigated region there are no prominent low-energy tetrahedral minima.

Among the group of neutron-rich  $Z = 84 - 94$  nuclei, there are altogether fourteen conditional minima below 2 MeV excitation energy: nine in Po isotopes, four in Rn isotopes, and in  $^{223}\text{Np}$ . An example of the energy landscape of a nucleus  $^{219}\text{Po}$ , with coexisting shallow, nearly degenerate minima: with  $\beta_{32} \approx 0.1$  and the wide prolate- $\beta_{30}$  one, is shown in Fig. 3, in three projections:  $(\beta_{20}, \beta_{22})$ ,  $(\beta_{20}, \beta_{30})$ , and  $(\beta_{20}, \beta_{32})$ . These maps were obtained by using all 10 deformations by the minimization over 8 remaining ones. The unusual landscape may be interpreted as two competing minima with a slight barrier between them.

Concerning the excited minima, the important question is whether they are protected by a barrier from the transition to the axially symmetric g.s. minimum. The typical situation is shown in Fig. 4, for the nucleus  $^{222}\text{Rn}$ . The landscape in  $(\beta_{20}, \beta_{32})$  plane was obtained by the minimization over 8 remaining deformations. One can see that the conditional minimum with  $\beta_{20} = 0$  is not a minimum after lifting the constraint on  $\beta_{20}$ : the very shallow real tetrahedral minimum

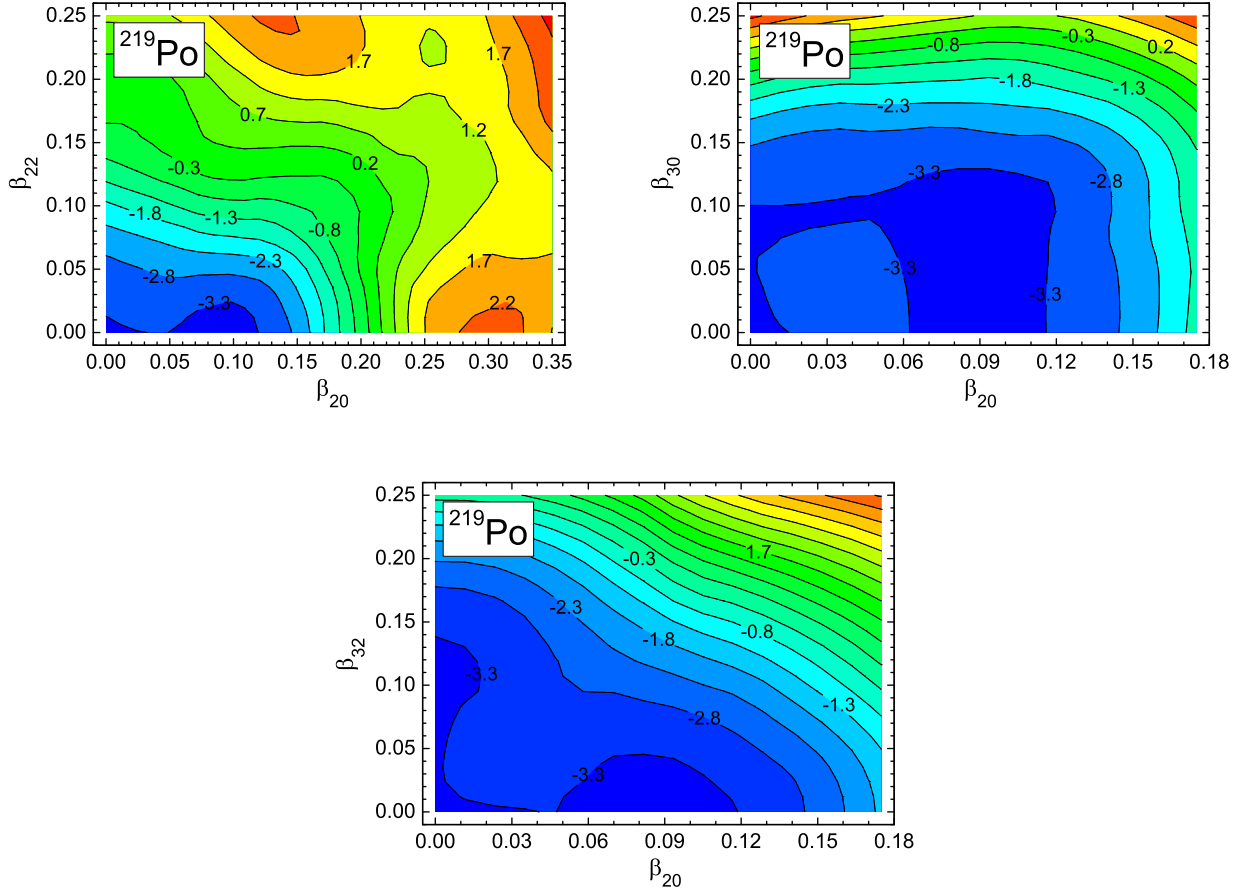


FIG. 3: (color online) Energy landscapes in  $(\beta_{20}, \beta_{22})$ ,  $(\beta_{20}, \beta_{30})$  and  $(\beta_{20}, \beta_{32})$  planes for  $^{219}\text{Po}$ , calculated from the minimization over the remaining eight deformation parameters. Energy calculated relative to the macroscopic energy at the spherical shape.

occurs at  $\beta_{20} = -0.04$  and  $\beta_{32} = 0.04$  which is smaller than  $\beta_{32} = 0.10$  of the conditional minimum. The barrier between the tetrahedral and the axial prolate g.s. minimum is less than 300 keV. One has to notice though, that the presented picture involves the minimization over other deformations, while finding the height of the saddle would require another method, like, for example, the imaginary water flow (e.g. [34, 35]), applied in the whole deformation hypercube.

### B. Minima including tetrahedral deformation

In the next step we found all nuclei in which the energy minimization over 10 deformations, including nonaxial  $\beta_{22}$ ,  $\beta_{32}$  and  $\beta_{42}$ , lead to the g.s. lying lower than the axially symmetric minimum. They are shown in Fig. 5. In many of them, the effect comes entirely from the quadrupole and hexadecapole nonaxiality ( $\beta_{22}$  and  $\beta_{42}$ ). Such is the situation in nuclei with  $Z < 118$ , forming vertical lines in Fig. 5: at  $N = 121, 179$  (nuclei with small oblate deformation  $\beta_{20} > -0.1$ ), and  $N = 137, 153$  (well deformed prolate nuclei with  $\beta_{20} \approx 0.25$ ). Among the last group, there are only a few cases in which a small deformation  $\beta_{32} \approx 0.02 - 0.03$  occurs in the g.s. On the other hand, in many nearly spherical  $N = 185$  isotones a small distortion  $\beta_{32} \approx 0.03$  results from the energy minimization. The energy differences greater than 200 keV between non-axial and axial minima occur in rather exotic nuclei. For example, the purely tetrahedral effect occurs in the neutron-poor Es isotope with  $N = 128$  neutrons and in ultra-neutron-rich Es isotopes with  $N = 185 - 192$ , and also in a few nuclei around them.

The largest effect occurs for SH nuclei with  $Z > 118$ , especially around  $Z = 123$ ,  $N = 173$ . In Fig. 6 are shown nuclei from this region in which the tetrahedral deformation  $\beta_{32}$  lowers the ground state by more than 150 keV. This effect is calculated as the difference between energies in the g.s. minimum from the minimizations including

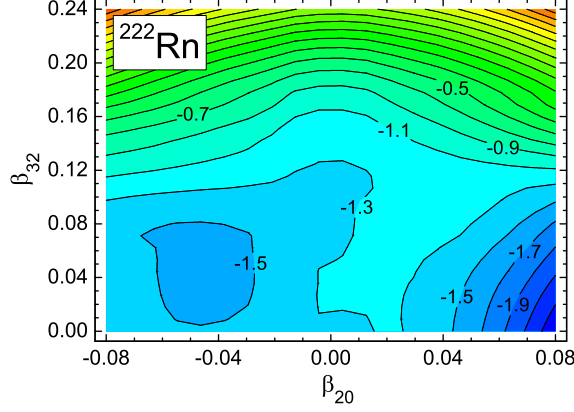


FIG. 4: (color online) Energy map for  $^{222}\text{Rn}$ ; only a small barrier may be seen between the slightly oblate,  $\beta_{32} = 0.04$  minimum and the axially symmetric g.s. with  $\beta_{20} \approx 0.12$  (not fully visible on this map).

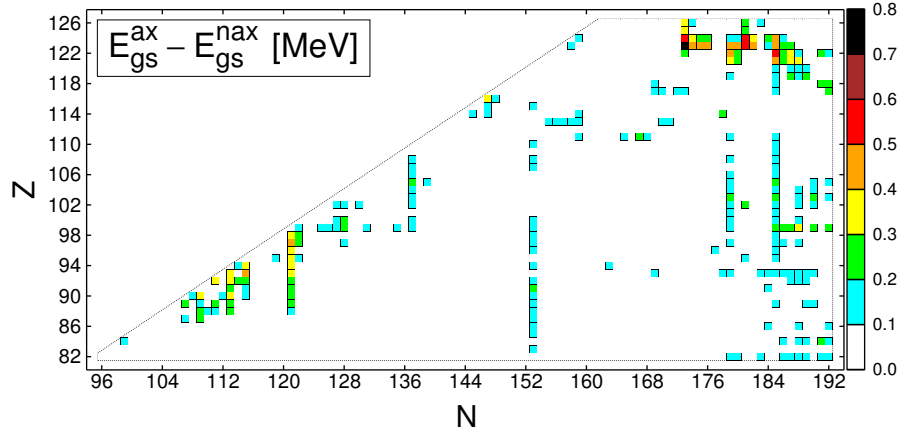


FIG. 5: (color online) Nuclei for which the minima obtained by using 10 deformations including quadrupole nonaxiality  $\beta_{22}$  and octupole  $\beta_{30}$  and  $\beta_{32}$  are below the axial ones.

nine (excluding  $\beta_{32}$ ) and ten (including  $\beta_{32}$ ) deformations. Although this could be named a "pure"  $\beta_{32}$  effect, the reality is more intricate. It turns out that including tetrahedral deformation induces also oblate quadrupole and the *axial octupole*  $\beta_{30}$ . The obtained minima, corresponding to moderately oblate shapes with octupole distortions in the ratio:  $\beta_{32}/\beta_{30} \approx \sqrt{3/5}$  are equivalent to the octupole deformation  $\beta_{33}$  superimposed on the oblate shape along its symmetry axis. A result of this superposition is an oblate spheroid with a slightly triangular equator. The minimum corresponding to such a nuclear shape was previously reported for  $^{308}\text{126}$  in [36]. In contrast to the case of  $^{308}\text{126}$ , some of the oblate- $\beta_{33}$  minima in nuclei depicted in Fig. 6 lie significantly lower than the oblate minima obtained when assuming the axial symmetry.

The landscapes around the g.s. minima in nuclei  $^{296}\text{123}$  and  $^{305}\text{124}$  are shown in Fig. 7 in three different projections:  $(\beta_{20}, \beta_{22})$ ,  $(\beta_{20}, \beta_{30})$  and  $(\beta_{20}, \beta_{32})$ . As previously, these maps are obtained by minimizing over the remaining eight deformation parameters. The oblate- $\beta_{33}$  minima are lower by 720 and 530 keV, respectively, than the axially symmetric oblate minima. As there is no barrier between both, the previously found axially symmetric minima were spurious.

One has to mention that the depth of the oblate- $\beta_{33}$  minima diminishes with increasing pairing strengths which is especially relevant in odd- $A$  and odd-odd nuclei. As we have checked, at least some of these minima survive even after a 10% increase in pairing strengths which corresponds to a considerable increase in rather weak g.s. pairing correlations of the original model. For example, such a change leads to the  $\beta_{33}$  g.s. in  $^{296}\text{123}$  still lying by 450 keV

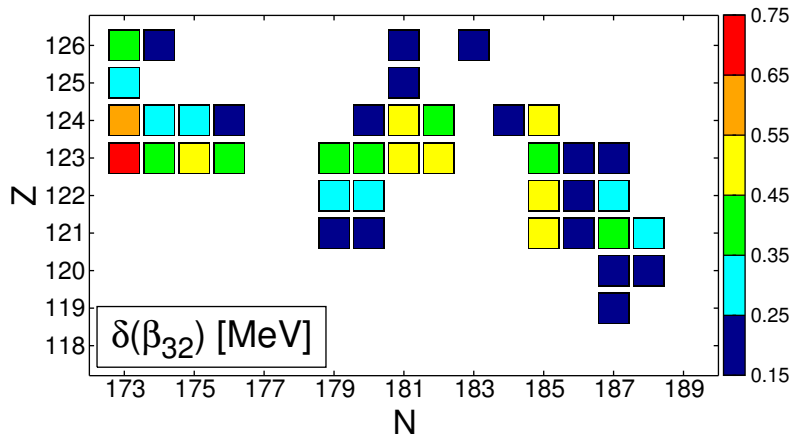


FIG. 6: (color online) Nuclei around  $^{296}_{123}$  for which the inclusion of  $\beta_{32}$  lowers the g.s. by at least 150 keV as compared to the minimization over nine deformations.

lower than the axially symmetric minimum.

#### IV. SUMMARY AND CONCLUSIONS

The results obtained for about 3000 heavy and superheavy nuclei by the microscopic-macroscopic model based on the deformed Woods-Saxon potential and the Yukawa-plus-exponential energy within the ten-dimensional space of deformations may be summarized as follows:

- We could not find any deep minima of large tetrahedral deformation. The conditional minima, found under the restriction of zero quadrupole distortion, have mostly a large excitation and are not protected by any substantial barrier. The g.s. minima relatively soft with respect to the tetrahedral coordinate  $\beta_{32}$  occur in Po isotopes with  $N \approx 136$  and in a few very exotic (off  $\beta$  - stability) systems.

- The tetrahedral deformation  $\beta_{32}$  appears in the g.s. minima when one combines it with  $\beta_{30}$  and allows simultaneously for the quadrupole nonaxiality  $\beta_{22}$ . Then it turns out that in  $\sim 40$  superheavy nuclei with  $Z = 119 - 126$ ,  $N = 173 - 188$ , the ground states have a combined oblate and octupole deformation of the  $\beta_{33}$  symmetry with respect to the axis of the oblate shape. The maximal g.s. lowering by this deformation, by 730 keV, occurs for the nucleus  $^{296}_{123}$ . The effect, although reduced (to 450 keV in  $^{296}_{123}$ ), survives in the calculation with 10% larger pairing strengths. This suggests some robustness of the prediction of oblate- $\beta_{33}$  ground states.

Summarizing, one may thus say that our search for tetrahedral minima lead us instead to finding a combined oblate-plus- $\beta_{33}$  g.s. deformation in a restricted region of superheavy nuclei.

#### Acknowledgements

M. K. and J. S. were co-financed by the National Science Centre under Contract No. UMO-2013/08/M/ST2/00257 (LEA COPIGAL). One of the authors (P. J.) was co-financed by Ministry of Science and Higher Education: Iuventus Plus grant nr IP2014 016073. This research was also supported by an allocation of advanced computing resources provided by the Świerk Computing Centre (CIŚ) at the National Centre for Nuclear Research (NCBJ) (<http://www.cis.gov.pl>).

- 
- [1] R. C. Lemmon et al., Phys. Lett. B **316**, 32 (1993).
  - [2] J. R. Leigh et al., Phys. Rev. C **52**, 3151 (1995).
  - [3] L. P. Gaffney et al., Nature **497**, 199 (2013).

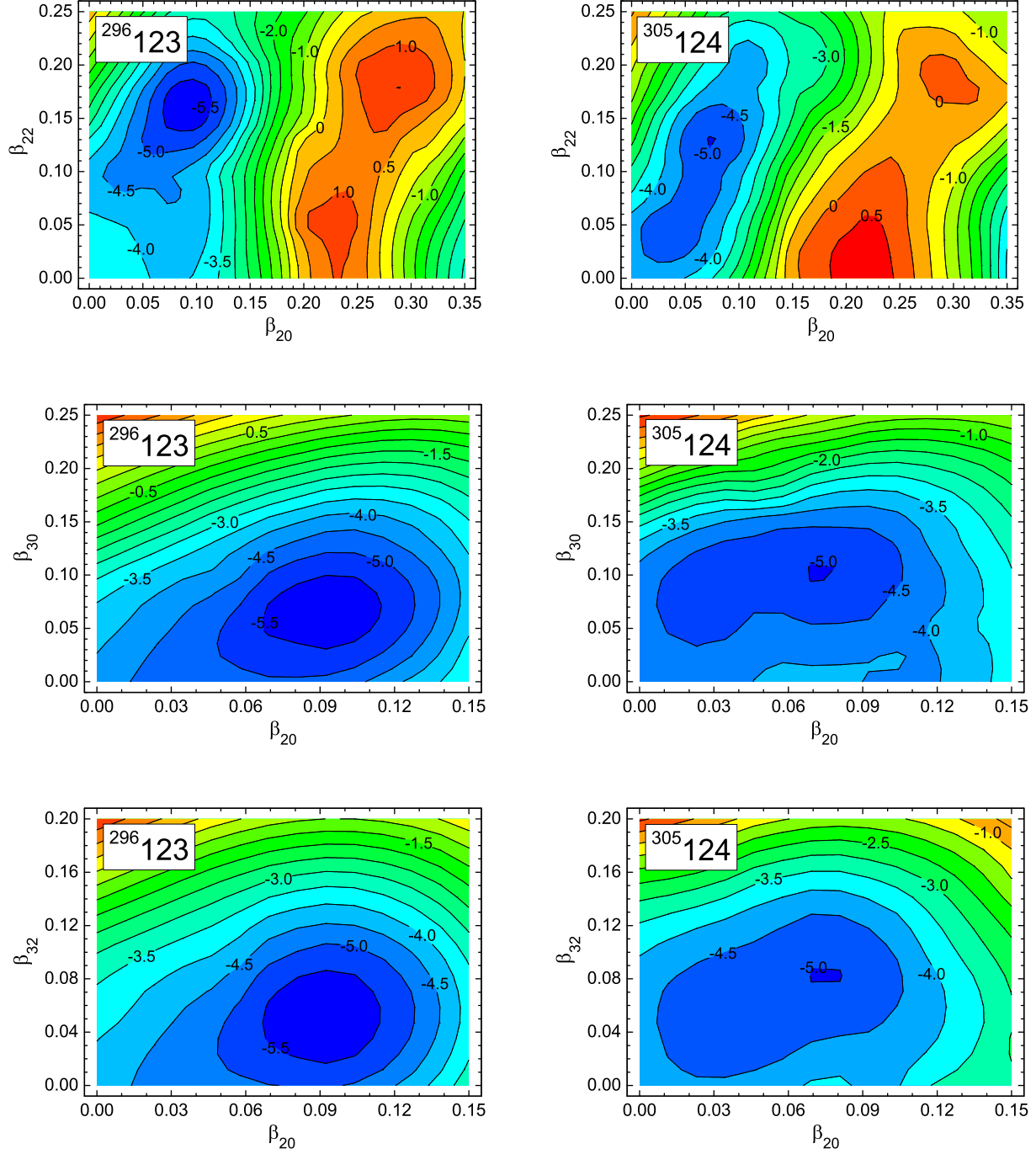


FIG. 7: (color online) Energy landscapes in  $(\beta_{20}, \beta_{22})$ ,  $(\beta_{20}, \beta_{30})$  and  $(\beta_{20}, \beta_{32})$  planes for nuclei:  $Z = 122$ ,  $N = 173$  and  $Z = 124$ ,  $N = 181$ , calculated from the minimization over the remaining eight deformations. Energy calculated relative to the macroscopic energy at the spherical shape.

- [4] B. Bucher et al., Phys. Rev. Lett. **116**, 112503 (2016).
- [5] P. A. Butler and W. Nazarewicz, Rev. Mod. Phys. **68**, 349 (1996).
- [6] P. Möller, R. Bengtsson, B. G. Carlsson, P. Olivius, and T. Ichikawa, Phys. Rev. Lett. **97**, 162502 (2006).
- [7] J. Skalski, S. Mizutori, and W. Nazarewicz, Nucl. Phys. A **617**, 282 (1997).
- [8] A. Obertelli et al., Phys. Rev. C **80**, 031304 (2009)
- [9] Y. Toh et al., Phys. Rev. C **87**, 041304(R) (2013)

- [10] N. Onishi and R. K. Sheline, Nucl. Phys. A **165**, 180 (1971).
- [11] D. Robson, Phys. Rev. Lett. **42**, 876 (1979).
- [12] I. Hamamoto, B. Mottelson, H. Xie, and X. Z. Zhang, Z. Phys. D **21**, 163 (1991).
- [13] X. Li and J. Dudek, Phys. Rev. C **49**, R1250 (1994).
- [14] N. Schunck, J. Dudek, A. Góźdz, and P. H. Regan, Phys. Rev. C **69**, 061305(R) (2004).
- [15] J. Dudek et al., Phys. Rev. Lett. **97**, 072501 (2006).
- [16] J. Dudek, A. Góźdz, N. Schunck, and M. Miskiewicz, Phys. Rev. Lett. **88**, 252502 (2002).
- [17] K. Mazurek, J. Dudek, A. Góźdz, D. Curien, M. Kmiecik, A. Maj, Acta Phys. Pol. B **40**, 731 (2009).
- [18] S. Takami, K. Yabana, and M. Matsuo, Phys. Lett. B **431**, 242 (1998).
- [19] M. Yamagami, K. Matsuyanagi, M. Matsuo, Nucl. Phys. A **693**, 579 (2001).
- [20] K. Zberecki, P. Magierski, P.-H. Heenen, and N. Schunck, Phys. Rev. C **74**, 051302(R) (2006).
- [21] K. Zberecki, P.-H. Heenen, and P. Magierski, Phys. Rev. C **79**, 014319 (2009).
- [22] J. Zhao, B. N. Lu, E. G. Zhao, and S.-G. Zhou, Phys. Rev. C **86**, 057304 (2012).
- [23] J. Zhao, B. N. Lu, E. G. Zhao, and S.-G. Zhou, Phys. Rev. C **95**, 014320 (2017).
- [24] P. Jachimowicz, P. Rozmej, M. Kowal, J. Skalski, and A. Sobiczewski, Int. J. Mod. Phys. E **20**, 514 (2011).
- [25] T. Sumikama et al., Phys. Rev. Lett. **106**, 202501 (2011).
- [26] R. A. Bark et al., Phys. Rev. Lett. **104**, 022501 (2010).
- [27] M. Jentschel et al., Phys. Rev. Lett. **104**, 222502 (2010).
- [28] D. J. Hartley et al., Phys. Rev. C **95**, 014321 (2017).
- [29] S. Ćwiok, J. Dudek, W. Nazarewicz, J. Skalski, and T. Werner, Comput. Phys. Commun. **46**, 379 (1987).
- [30] H. J. Krappe, J. R. Nix and A. J. Sierk, Phys. Rev. C **20**, 992 (1979).
- [31] I. Muntian, Z. Patyk and A. Sobiczewski, Acta Phys. Pol. B **32**, 691 (2001).
- [32] M. Kowal, P. Jachimowicz, A. Sobiczewski, Phys. Rev. C **82**, 014303 (2010).
- [33] P. Jachimowicz, M. Kowal and J. Skalski, Phys. Rev. C **85**, 034305 (2012).
- [34] P. Jachimowicz, M. Kowal and J. Skalski, Phys. Rev. C **95**, 014303 (2017).
- [35] P. Möller, A. J. Sierk, T. Ichikawa, A. Iwamoto and R. Bengtsson, Phys. Rev. C **79**, 064304 (2009).
- [36] P. Jachimowicz, M. Kowal, and J. Skalski, Int. J. Mod. Phys. E **19**, 508 (2010).